10

Live Cells as Optical Fibers in the Vertebrate Retina

Andreas Reichenbach[1], Kristian Franze[1,2], Silke Agte[1,3], Stephan Junek[4], Antje Wurm[1], Jens Grosche[1], Alexej Savvinov[5], Jochen Guck[2] and Serguei N. Skatchkov[5]
[1,3]*Leipzig University;*
[2]*Cambridge University;*
[4]*Max Planck Institute for Brain Research, Frankfurt/M.;*
[5]*Universidad Central del Caribe, Bayamon;*
[1,3,4]*Germany*
[2]*UK*
[5]*Puerto Rico*

1. Introduction

The vertebrate eye is equipped with an inverted-type retina; that means, light must pass through all proximal retinal layers before it arrives at the photoreceptor cells which are aligned at the back of the tissue. Though it is often stated that the transparency of the intact vertebrate retina is 'almost total' (Enoch and Glisman, 1966), it contains numerous structures which differ in size and refractive index. These differences should lead to significant scattering. Accordingly, it has been pointed out that the situation in the inverted retina 'is equivalent to placing a thin diffusing screen directly over the film in your camera' (Goldsmith, 1990). In fact, many current digital cameras posses such a "diffusing screen", in order to prevent artifacts due to the discrete and periodic sampling of the image: the anti-aliasing filter. As the layout of the retina exhibits a similar sampling strategy, one might hypothesize that the cell layers in front of the photoreceptors act as an anti-aliasing filter. However, the fact that aliasing artifacts can be observed in the vertebrate eye (Coletta et al. 1990) argues against such a hypothesis. On the contrary, these reports confirm the high resolution provided by the vertebrate retina, close to its physical limits. We will discuss here whether this apparent discrepancy is resolved by the presence of cellular light guides within the retinal tissue.

2. The inverted vertebrate retina: optical properties of the tissue

Before going into more detail, the basic structure, phylogenetic origin, and embryonic development of the vertebrate retina will briefly be introduced.

2.1 Basic morphology of the vertebrate retina

The retina has a well-organized structure with seven main layers (Fig. 1). Three layers contain the cell bodies with the cell nuclei (outer nuclear layer, ONL; inner nuclear layer,

INL; ganglion cell layer, GCL), two layers, connecting the nuclear layers, contain cellular processes and the neuronal synapses (the outer plexiform layer, OPL, and the inner plexiform layer, IPL), the innermost layer contains the axons of the ganglion cells on their course towards the optic nerve head (nerve fiber layer, NFL), and the outermost layer is formed by the photoreceptor segments (PRL). The neural retina can be divided into an inner and outer part. The inner retina includes the NFL, GCL, IPL, and INL, and the outer retina consists of the OPL, ONL, and PRL (Fig. 1).

There are three types of neurons that lie in series and mediate the forward transmission of the visual information from the photoreceptor outer segments (where light is absorbed by the photosensitive pigments) at the outer surface of the neural retina to the axons at the inner surface of the retina running towards the optic nerve. These are, (i) the photoreceptor cells (the first-order neurons of the retina), (ii) the bipolar cells (the major second-order neurons, which are also called interneurons), and (iii) the ganglion cells (the third-order neurons, also called projection neurons). Photoreceptor cells consist of three parts: the soma of the cell, containing the cell nucleus, is located in the outer nuclear layer; the sensory process that consists of an inner segment (containing the energy-producing mitochondria) and an outer segment (containing the molecular machinery that captures the photons and converts the light energy into neuronal activity); and an axon which forms synapses with the bipolar cells (and other interneurons) in the outer plexiform layer. There are two basic types of photoreceptor cells, rods (responsible for the low contrast, 'black-and-white', but high sensitivity vision at low light intensities; scotopic vision) and cones (responsible for high contrast and color vision at bright daylight; photopic vision).

In addition to these neurons, elongated 'radial' glial cells span the entire thickness of the tissue; these are called Müller cells. As shown in Figure 1, a distinct set of retinal neurons is aligned along each Müller cell, thus forming a so-called columnar unit (Reichenbach et al., 1994; Reichenbach and Robinson, 1995). Basically, a vertebrate retina can thus be considered as being composed of a large number (almost 10.000.000 in the human eye) of such repetitive columnar units, each contributing its part to the visual information collected by the retina. The constituents of a columnar unit are remarkably constant across a given retina and largely independent of local topographic specializations (there are some exceptions such as the primate fovea centralis). However, the cellular composition of the columnar units differs considerably among the diverse vertebrates, even among mammalian species; this depends mainly on the diurnal *vs*. nocturnal lifestyle, i.e., the photopic *vs*. scotopic specialization of the retina (cf. section 4.3). In all mammals studied so far, every unit contains, in addition to the 'core Müller cell', (i) about 1 cone plus a variable number of rods, (ii) at least three interneurons of the INL, and (iii) one or two ganglion cell(s) in photopically specialized retinas (or less than one in the other retinas).

2.2 Phylogenetic origin and embryonic development of the vertebrate retina

During both phylogenesis and embryonic development, the retina of all vertebrates emerges from the same primitive neural tissue (the 'neural plate') as the brain does; it is thus considered as an 'externalized' part of the brain. To understand the inversion of the vertebrate retina, it is essential to keep in mind that vertebrates belong to the deuterostomian animals which means that our ancestors belong to the relatives of recent starfish and sea urchins. The starfish possesses an epithelial nervous system. It locally constitutes the outer surface of the body, where it directly contacts the seawater as a fluid environment, with a basal lamina deliminating the epidermal tissue at the inner side. It

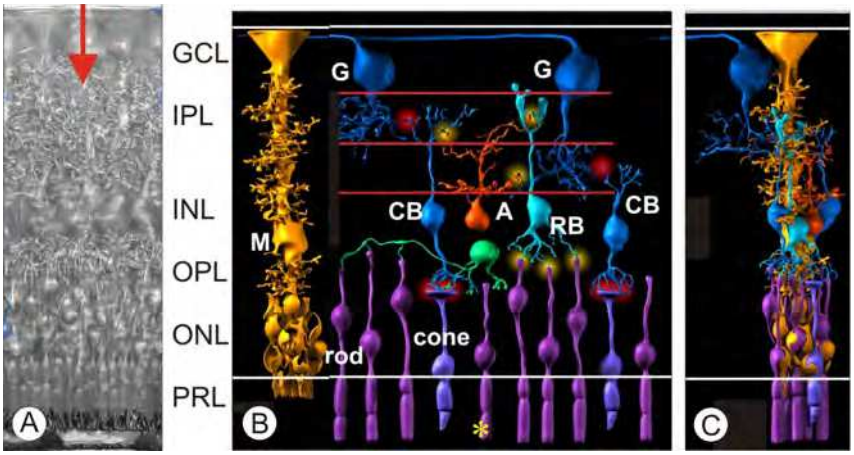

Fig. 1. Structural composition of a typical vertebrate retina; artists view. (A) Radial section through a mammalian retina with the typical layers. (B) The concept of columnar units in the vertebrate retina. The tissue is built up by a large number of repetitive groups of cells which are arranged in columns (C). The center of each column is constituted by a Müller cell (M) which extends lateral side branches ensheathing the adjacent neurons of the unit. G, retinal ganglion cell; B, bipolar cells; A, amacrine cell. Each column spans all retinal layers (GCL, ganglion cell layer; IPL, inner plexiform layer; INL, inner nuclear layer; OPL, outer plexiform layer; ONL, outer nuclear layer). The inner and outer segments of the photoreceptor cells reside in the photoreceptor layer (PRL). Original.

contains so-called supporting cells – which can be considered as the ancestors of radial glial cells (Reichenbach and Robinson, 1995) and two principal types of neurons. The sensory processes of the sensory cells extend into the maritime environment as the source of the stimuli to be monitored, whereas their axons reach towards the ganglion cells where the information is processed. Notably, this polarity is obviously 'correct' and easily comprehensible.

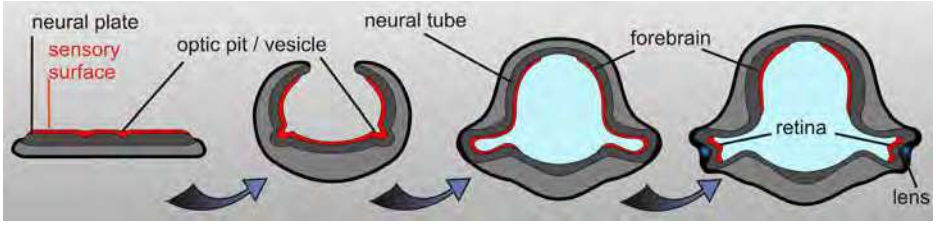

Fig. 2. Developmental mechanism causing the inversion of the vertebrate retina. Embryonic development of the retina occurs by evagination of the eye anlage (optic pit / vesicle) from the neural epithelium (from *left* to *right*). Later on, the outer wall of the optic vesicle becomes invaginated by the developing lens. This outer wall differentiates into the neural retina whereas the inner wall becomes the retinal pigment epithelium; the stalk is transformed into the optic nerve. Initially the 'sensory surface' (*red*) constitutes the outer surface of the neural plate (and the embryo); however, it becomes translocated into the inner surface by the invagination of the neural tube.

In the further course of evolution, the epithelial nervous system was maintained as such, but was enrolled into a tube and moved below the surface of the body by the overfolding or overgrowing skin and subepidermal layers. Similar events occur during our embryogenesis when the – originally superficial - neural plate is enrolled and overlayed in a process called neurulation (Fig. 2). Inevitably, this mechanism is accompanied by an inside-out turn of the polarized epithelium: the sensory cells which had faced the environment at the surface of the body now extend their sensory processes into the lumen – i.e., the inner surface - of the neural tube. This also explains for the 'odd' orientation of our retina (Fig. 1), with the photoreceptor cells directed away from the light. During the evagination of the optic vesicle from the neural tube the 'sensory surface' remains at the inner, 'wrong' surface (Fig. 2). Thus, the normal developmental mechanisms of our eyes inevitably lead to an inverted retina.

2.3 General optics of the retinal tissue

It has long been known that there is considerable light scattering in the retina which constitutes a 'turbid medium' (Boehm, 1940b) contributing up to 40% to entopic light scatter (Vos & Bouman, 1964), and allowing for a light transmission of only 85% at 500 nm (Hammer et al., 1995). Whereas a freshly isolated retina appears virtually transparent when viewed from top (i.e., orthogonally to its surface; see *arrow* in Fig. 3B) it looks 'milky' if one looks obliquely on the tissue (which tends to enrol) (Fig. 3).

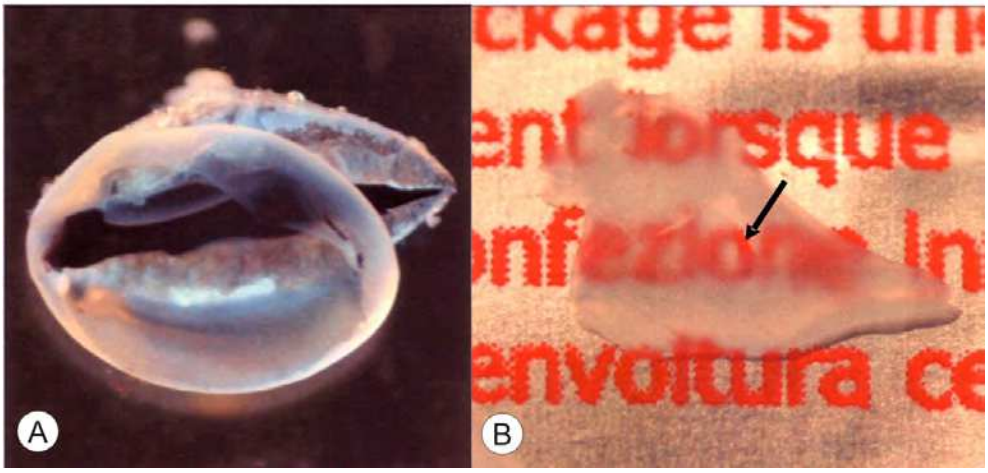

Fig. 3. Limited transparancy of the vertebrate retina. (A) Freshly dissociated guinea-pig retina in a buffer-filled Petri dish over a black background. (B) A piece of the same retina over some text. Only where the tissue is flat over a letter, the letter can be read easily (*arrow*). Wherever the retinal tissue is somehow enrolled and light incidence is thus not normal to the surface, the image is blurred.

It has also become evident that light scattering is inhomogenous among the retinal layers; particularly strong light scatter has been located in the inner plexiform layer (Martins-Ferreira & de Oliveira Castro, 1966) and in axon bundles of the nerve fiber layer (Knighton et al., 1989). Much of this scatter is due to small subcellular elements with dimensions in the order of the wavelengths of visible light (Boehm, 1940; Knighton et al., 1989; de Oliveira Castro et al., 1985) such as neurofilaments, neurotubuli, and other organelles which are enriched in the nerve fiber and plexiform (i.e., synaptic) layers. This scattering is, for example, used to visualize (some of the) individual retinal layers in intact eyes of human patients by optical coherence tomography (OCT) (e.g., Puliafito et al., 1995) (Fig. 4).

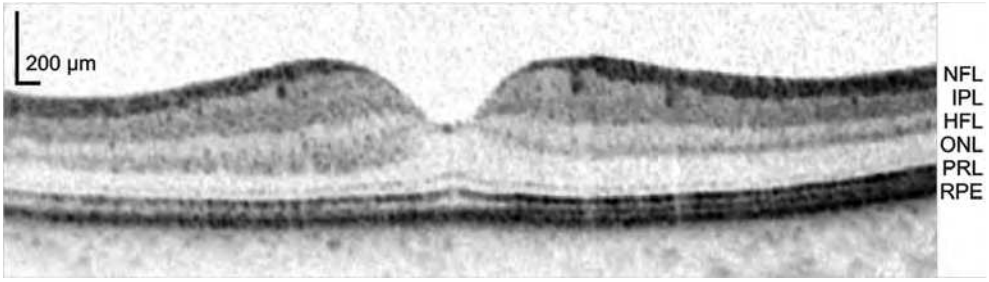

Fig. 4. Optical coherence tomography (OCT) demonstrates differential backscattering of light from human retina.

When a human retina in the intact patient's eye is studied by OCT, most of the retinal layers are easily identified because of the different amount of their backscattering of the laser. The cell process-containing layers (NFL, IPL, and HFL) display more backscattering (dark) than the cellular layers. NFL, nerve fiber layer; IPL, inner plexiform layer; HFL, Henle's fiber layer; ONL, outer nuclear layer; RPE, retinal pigment epithelium.
In fact, the refractive index of the retinal tissue is higher (about 1.36) (Chen, 1993; Valentin, 1879; Nordenson, 1934; Ajo, 1949) than that of the vitreous (1.336) (Nordenson, 1934). This causes a specular reflection from the retinal surface (Millodot, 1972; Charman, 1980; Gorrand, 1986) which may contribute to about half of the light leaving the eye, and which causes the 'fundus reflexes' familiar to ophthalmoscopists. It can be summarized that the retina is all but perfectly transparent; later we will show data revealing even different refractive indices among retinal cell types (sections 3.1, 4.1, 4.2).

2.4 Performance of the vertebrate retina

Despite these considerations, most vertebrates including humans can reliably detect a light signal when only a few photons enter the eye (Pirenne, 1967). Moreover, our visual acuity - even outside the *fovea centralis* where the inner retinal layers are missing – is as good as the spacing of two neighboring cone photoreceptor cells allows, resulting in the highest possible resolution (Livingstone and Hubel, 1988; Williams et al., 1993). This has stimulated the search for a mechanism that may minimize intraretinal light scatter.

3. Methods to study cell and tissue optics of the vertebrate retina

In order to understand the pathway of light through the inverted vertebrate retina it is essential to collect precise data about the optical properties of the retinal tissue and of its

constituents, the retinal cells. Whereas first measurements of retinal optics date back to the late 19th century, many methods only became available in recent years. The following sections are aimed at providing an overview of 'traditional' and current techniques that have been employed, or may be employed, to study retinal optics down to the cellular level.

3.1 Assessing the refractive index of single cells and retinal tissue

There are different indirect and direct approaches to determine the *refractive index n* (RI) of living tissues and individual cells.

In historical experiments, Valentin used a refractometer to measure the RI of different types of biological liquids and tissues of different species including retinae (1.3411 (rabbit) ≤ n ≤ 1.3461 (young chicken) (Valentin, 1879)). However, this technique assesses the refraction angles at parallel interfaces, which are rarely found in biological tissues. Nerve tissue, for example, had to be crushed to a mushy mass in order to provide reproducible results. Furthermore, this method only yields an average value for the RI of the whole sample.

The RI of biological samples can be taken as a measure of the total organic solids present (which is mostly determined by the protein concentration) (Barer, 1954). Based on their total dry mass concentration, Chen estimated the RI of individual retinal layers to be between 1.369 and 1.358 (Chen, 1993). The ratios of the refractive indices of neighboring retinal layers were similar.

Furthermore, the RI of individual, acutely isolated cells can, for example, be determined with an index matching method. Here, cells are sequentially exposed to a series of isotonic superfusates of graded RI, which are adjusted to a value at which most of the cells become virtually invisible in phase contrast microscopy. One way of obtaining solutions with higher RI is by adding different concentrations of bovine serum albumin (BSA). This technique is comparable to the immersion method established in mineralogy and crystallography. However, it is difficult to raise the RI of the medium to higher values without damaging vital cells, and all of the above-mentioned approaches suffer from relatively poor resolution.

More sophisticated setups to measure the RI of biological samples with high spatial resolution include Jamin-Lebedeff microscopes (Franze et al., 2007) and digital holographic microscopy (DHM) (Charriere et al., 2006). These methods exploit interference microscopy, which can be used to quantitatively determine optical pathway differences. The optical path difference depends on both the RI and the thickness of the sample (the phase profile represents the multiplication of RI differences and sample thickness). Thus, the refractive index itself cannot be measured without determining the thickness of the cells separately. This determination is often subject to considerable errors. Methods to decouple the RI from the cell thickness include a combination of interference microscopy with confocal laser scanning microscopy or atomic force microscopy (the latter methods are used to measure the sample height) as well as measuring the phase profiles of the same sample in media with different RIs. In case of cells in solution, exact three-dimensional tomographical image can be obtained with a dual-beam laser trap-based optical cell rotator (Kreysing et al., 2008).

3.2 Measuring light propagation through individual cells

Light transmission through retinal cells can be observed '*in situ*', i.e., while the cells are within the intact retinal tissue. This way, light exiting the distal light path, i.e., the photoreceptor outer segments, can be visualized. Pioneering experiments by Enoch and

Tobey in the 1960s and 1970s suggested that the outer segments of photoreceptor cells act as "light collectors" (Tobey et al., 1975) and wave guides. Light transmission through these outer segments *in situ* occurs in modal patterns as known from optical fibers (Enoch, 1961). The most commonly seen modes included HE_{11}, TE_{01}, and TM_{01} (Enoch, 1961) (Fig. 5). In some of the observed cells, mode changes occurred with changing wavelength.

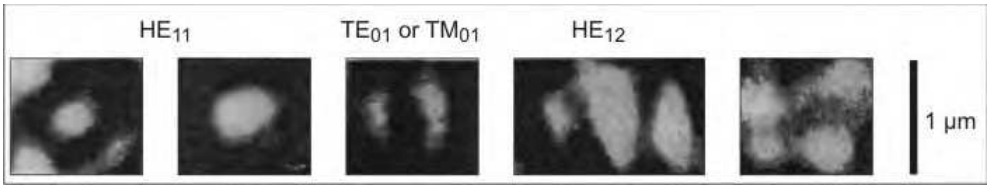

Fig. 5. Modal patterns of light exiting photoreceptor cell outer segments of rhesus macaque monkeys. Scale bar: 1 µm. (adapted from Enoch, 1961).

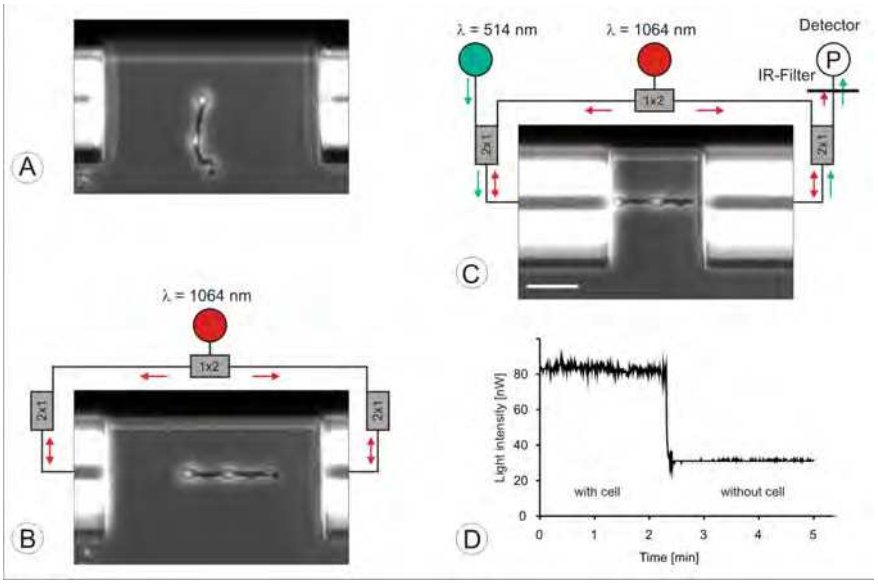

Fig. 6. Individual Müller cells as optical fibers. Demonstration of light guiding properties of individual Müller cells measured in a modified dual-beam laser trap. **A,** A cell is floating freely between the ends of two optical fibers, which are aligned against a backstop visible at top. **B,** The Müller cell is trapped, aligned, and stretched out by two counter-propagating infrared (IR)-laser beams (λ = 1064 nm; not visible in the image) diverging from optical fibers. **C,** The fibers are brought in contact with the cell. Blue light (λ = 514 nm) emerges from the left optical (input) fiber, and is collected and guided by the cell to the right (output) fiber. The fraction of blue light re-entering the core of the output fiber is measured by a powermeter, while the IR light is blocked by an appropriate cut-off filter. Scale bar, 50 µm. **D,** Typical time course of the power of the blue light measured. When the cell is removed from the trap, only a fraction of the blue light, which is no longer confined to the cell but diverges freely, is measured. The ratio $P_{\text{cell}} / P_{\text{no cell}}$ defines the relative guiding efficiency.

Franze et al. developed a setup to investigate light transport through individual cells that are located proximally to the photoreceptors (i.e., closer to the inner retinal surface) (Franze et al., 2007) (Fig. 6). Enzymatically dissociated retinal cells were optically trapped between the ends of two opposing optical fibers (single-mode at 1064 nm) by counter-propagating infrared laser beams (Ytterbium fiber laser, λ = 1064 nm). The refractive index of the cell medium has been elevated to that of retinal neurons (n ~ 1.36) by adding BSA (cf. chapter 3.1). Additionally, visible laser light (Argon Ion laser, λ = 514 nm) was coupled into one of the fibers, and the intensity of light coupling into the opposite fiber was measured. When the optical fibers are moved apart, only a fraction of the visible light emanating from one fiber couples into the opposing one, because of its divergence (Bass, 1995). However, when a structure capable of guiding light and thus preventing it from diverging is trapped, the intensity loss is minimized (Fig. 6).

3.3 Measuring the transmission and reflection of light on retinal tissue

Obtaining reliable quantitative data on light transmission and reflection of intact retinal tissue is a difficult task. Experiments have been carried out on bovine retina samples in a special setup (Fig. 7) with subsequent mathematical evaluation of the data (Hammer et al., 1995). Basically, the setup consisted of two integrating spheres (coated with barium oxide) between which the retinal sample was placed in the path of monochromatic light. Four detectors measured the light intensities at the start and end of the light path, and the scattered light collected within the integrating spheres (Fig. 7).

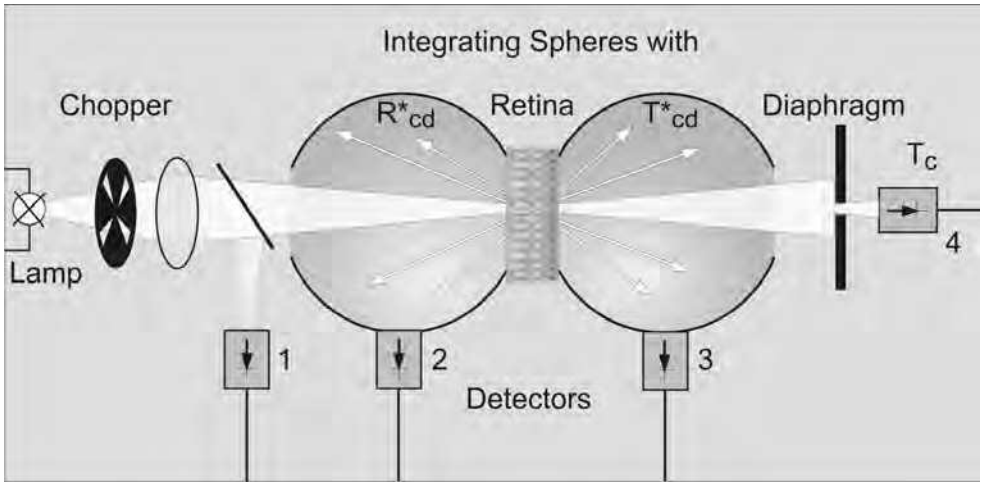

Fig. 7. Setup used to measure light transmission through and reflection at retinal tissue (modified from Hammer et al., 1995).

The calculation of optical tissue parameters involved three steps including an inverse Monte Carlo simulation. This approach revealed that, at λ=500nm (i.e., in the visible range of light), the retina transmits less than 90% of incident light, due to about 7% absorption and about 5% reflection (Hammer et al., 1995).
The retinal sample is placed between two integrating spheres which allow to collect light lost from straight transmission by diffuse reflectance (R^*_{cd}) and diffuse transmittance (T^*_{cd}). R^*_{cd} and T^*_{cd} were measured by two photodiodes (detectors 2 and 3, respectively). Furthermore, the incident light and the collimated transmittance (Tc) were measured by detectors 1 and 4, respectively. Light was provided by a xenon-high pressure lamp with monochromator.

3.4 Visualization of backscattering of light within retinal tissue by confocal microscopy

The retina contains numerous cellular structures (phase objects) with varying RI and sizes on the order of the wavelength of visible light. These structures should lead to significant scattering. Back-scattering can be visualized by detecting the reflection of (monochromatic) light that is sent through the tissue. Confocal microscopy offers a convenient way for such a measurement (Franze et al., 2007). An additional advantage of this approach is the possible three-dimensional reconstruction of optical slices, revealing the distribution of intensities of back-scattered light along the light path (cf. Fig. 11). Another technique that exploits the back-scattered light within a retina is optical coherence tomography (cf. Fig. 4).

3.5 Visualization of light propagation through the retinal tissue

To simulate the physiological light path in the inner retina, Franze et al. illuminated the retinal surface by light exiting a multimode optical fiber, which was inserted into a freshly dissected eye cup (Fig. 8A) (Franze et al., 2007). At the opposing side, the sclera, the choroid, the pigment epithelium and the photoreceptor cells were surgically removed, which allowed access to the end of the retinal light path with a confocal microscope. This approach revealed that the light transport through the inner retina is inhomogeneous (Fig. 8A).
To study the light transmission through the whole retina, a single mode optical fiber was mounted vertically above the inner surface of a retina (Fig. 8B). A micromanipulator was used to move the fiber in defined steps along the retinal surface, and the position of illuminated photoreceptor groups at the opposing side of the retina was recorded and compared to the fiber position (Fig. 8B) (Agte et al., 2011).
For a direct visualization of the light path within the retina, confocal microscopy of retinal cross-sections was combined with an optical fiber setup (Fig. 8C). Retinal slices were adhered to a nitrocellulose membrane, and Müller glial cells stained with a fluorescent dye. Green laser light exiting a single mode optical fiber was used to illuminate individual Müller cell endfeet. The fluorescence signal of Müller cells was recorded by one channel, the forward-scattered light was detected by another channel of the confocal microscope. Transmitted light was scattered in the filter membrane and could thus also be detected. An overlay of the channels allowed the detection of changes in light scattering as a function of changes in the fiber position relative to Müller cell positions (Fig. 8C). These experiments suggested that light hitting a Müller cell is guided more efficiently through the retinal tissue.

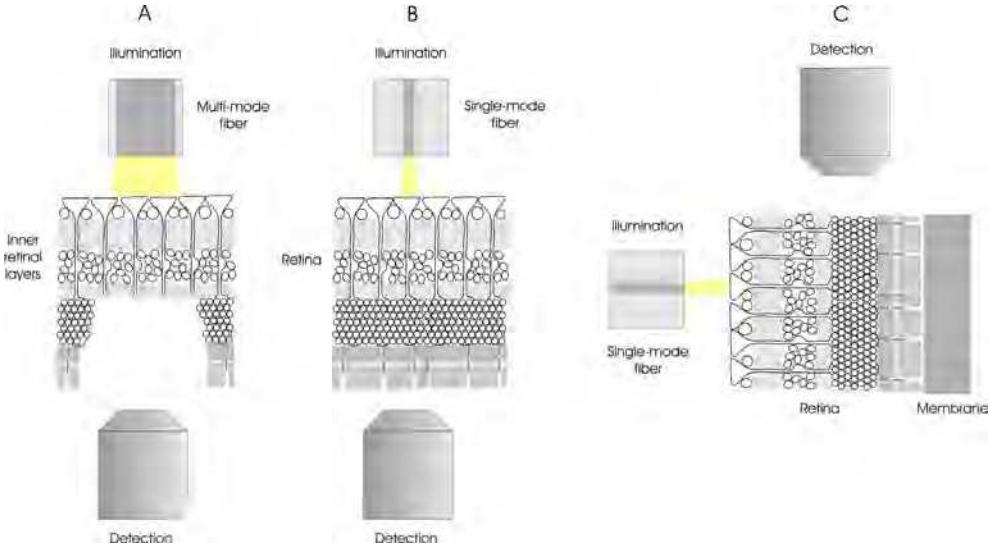

Fig. 8. Schemata of the illumination methods used to study the light transport through the retina. (A) The retina is placed on the stage of an inverted confocal microscope after surgically removing the photoreceptor cells. A multimode optical fiber provides a wide-field illumination of the retinal surface. The confocal microscope scans a plane close to the outer plexiform layer and monitors the light transmission through the inner retina. (B) To investigate the light distribution through the whole tissue, a single mode optical fiber is used to simulate the physiological illumination of individual Müller cells. An objective of an inverted microscope detects the light after passing all retinal layers. (C) A retinal slice is fixed on a nitrocellulose membrane and placed on the stage of an upright confocal microscope. A fluorescent staining visualizes Müller cells. The single mode fiber is positioned in front of individual Müller cells. Light scattering within the retinal cross-section is detected by the microscope. Light transmitted through the retina is visualized by monitoring the scattering in the membrane to which the retina is attached.

3.6 Physical and mathematical simulation

Assuming that total light reflection occurs in (outer and inner segments of) photoreceptor cells, light transport through the cells can be simulated by employing model 'cells' magnified into the microwave spectrum (Jean and O'Brian, 1949). Although only indirect evidence can be obtained, this magnification and the use of custom-made models allow a wide variation of parameters, and provide basic insights into the mechanisms involved.

The light path through cells and tissue compartments can also be simulated based on experimental data and appropriate physical models. Assuming that (certain) retinal cells are wave guides, the V parameter can be used to estimate the efficiency of light guidance. This method has been applied to (outer and inner segments of) photoreceptor cells (Enoch and Tobey, 1978) as well as to Müller glial cells (Franze et al., 2007). This parameter of a circular dielectric waveguide is given by the expression

$$V = (\pi d/\lambda)\ (n_1^2 - n_0^2)^{1/2},$$

where d is the diameter of the guide, λ is the wavelength in vacuum, and n_1 and n_0 are the indices of refraction of the inside (cell) and outside (surrounding) of the fiber, respectively. Generally, a cell can be considered as an efficient waveguide if $V > 2$ (cf. Fig. 10).
Using the same basic optics (and assuming that light propagates in the cells by total reflection), the light collecting (or light radiating) properties of non-cylindrical (paraboloid of revolution, cone-like) cell structures can be estimated (Winston and Enoch, 1971; Miller and Snyder, 1973) (cf. Fig. 9). It should be noted however, that this older theoretical view of light propagation with ray optics in mind is not really appropriate to describe the light transport through structures that are comparable in size to the wavelength of light propagating through them.

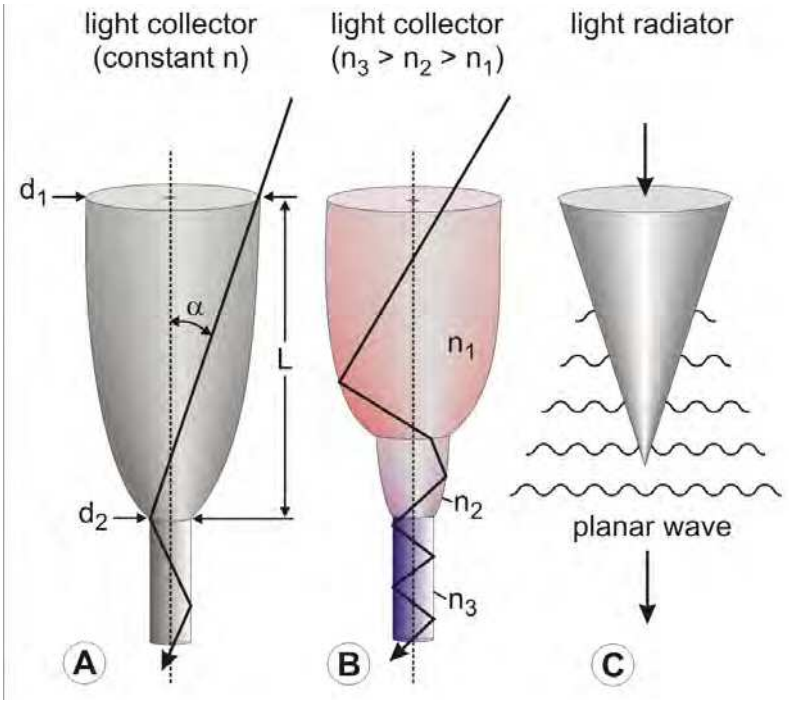

Fig. 9. Models for light collection (**A**, **B**) and light radiation (**C**) by (cone) photoreceptor cells. Incident light may be collected by a parabolic structure if its refractive index (n) exceeds that of its microenvironment (light collector: (**A**)). The accepted input semi-angle **α** can be estimated from morphological data (length **L** and larger - $\mathbf{d_1}$ - and smaller - $\mathbf{d_2}$ - diameter) and from refractive index differences ($\mathbf{n}_{object} - \mathbf{n}_{environment}$). The light collector can be 'improved' (i.e., **α** can be increased) if **n** increases along the light path (**B**). Both types of light collection have been ascribed to cone inner segments (ellypsoids) (Miller, 1981). By contrast, tapering cylinders may function as light radiators from which light spreads as a planar wave (**C**). It has been suggested that this applies to peripheral human cone outer segments which thereby may help to distribute light to the rod outer segments (Miller and Snyder, 1973). Modified from Winston and Enoch, 1971 (light collectors) and Miller and Snyder, 1973 (light radiator).

Numerical finite-difference time-domain and an analytic Mie theory approaches have been applied to model light transport through photoreceptor cell nuclei of diurnal and nocturnal animals in two and three dimensions (Solovei et al., 2009, Kreysing et al. 2010). These simulations revealed that, while the specific chromatin arrangements have little impact on the far-field scattering cross-section, scattering in the near field (which is the relevant regime inside the retina) shows a significant difference between retinae of diurnal and nocturnal animals. The "inverted" photoreceptor cell nuclei of nocturnal mammals have been suggested to act as collection lenses, which could improve night vision (cf. chapter 4.3).
Finally, Labin and Ribak recently used a direct three-dimensional numerical solution of the Helmholtz equation (the fast Fourier transform split-step beam propagation method of the global third order) to obtain a description of a propagating electromagnetic (EM) field along retinal cells and their vicinity (ref.). They confirmed that Müller glial cells preserve the acuity of images in the retina (Franze et al., 2007).

4. Experimental evidence for the presence of cellular optical fibers in the retina

The application of the above-mentioned experimental and theoretical approaches to retinal tissue samples and isolated retinal cells has shown that

- light propagation through – and light reflection by – the retina is non-homogenous;
- pronounced back-scattering of light occurs in the two plexiform layers, and in the nerve fiber layer;
- all layers are spanned by regularly arranged 'tubes' displaying low backscattering of light;
- these tubes were shown to be Müller cells, by vital dye filling and immunohistochemistry;
- isolated vital Müller cells display higher refractive indices than retinal neurons;
- these Müller cells provide efficient laser light guidance if interposed between glass fibers;
- in intact retinal tissue, Müller cells effectively guide light from vitread retinal surface to the photoreceptor cells;
- photoreceptor cell nuclei of nocturnal animals likely serve as densely packed arrays of microlenses;
- if hit by light, the photoreceptor cells themselves provide efficient light guidance towards their outer segments where the photosensitive molecules are located.

The following sections will highlight particular aspects of this knowledge, as it was accumulated over the years.

4.1 The 'classics': photoreceptor outer (and inner) segments are wave guides

It has been shown already in the mid 20th century that vertebrate photoreceptor cells display the properties of wave guides. In a comparative study, Sidman (1957) showed that various vertebrate rod outer segments display solid concentrations of 40-43%, and refractive indices of 1.4056 to 1.4106 whereas these values in cone outer segments were slightly lower (29.7 to 34.9% and 1.365 to 1.3958, respectively). These data suggested that photoreceptor cells can function as 'classical' wave guides, and light transmission through these cells occurs in modal patterns (Enoch, 1961; Tobey et al., 1975) (cf. Fig. 5).

Similar direct evidence for the wave guide properties of photoreceptor inner segments is missing, but the results of physical and mathematical simulations (cf. section 3.6) strongly suggest that light guidance also occurs in these inner segments. Moreover, based on mathematical simulations it was suggested that cone inner segments are light collectors, with an entrance aperture θ_{max} of 13° (Winston and Enoch, 1971) (cf. Fig. 9A). Taking into account that cone inner segments consist of several consecutive compartments (myoid, paraboloid) with different distinct refractive indices, a more complex simulation indicated that these inner segments of cones are ideal light-collectors with an even increased acceptance angle (Winston and Enoch, 1971) (cf. Fig. 9B).
In summary, it is now generally accepted that photoreceptor outer (and inner) segments are wave guides, and that (parts of cone) inner segments are light collectors funneling the light into the outer segments. Until very recently, however, it was unclear how sharp images can arrive at the 'apertures' of the inner segments.

4.2 The 'news': Müller glial cells are light guides that bridge the light-scattering elements in the inner retina

Whereas the healthy vertebrate retina appears very transparent if viewed from top (Fig. 4), it becomes turbid and acquires a 'milky' appearance when the Müller cells swell during 'spreading depression' (a condition involving extreme changes in intra- and extracellular ion concentrations) (Gouras, 1958; Mori et al., 1976; van Harreveld 1984; De Oliveira Castro et al., 1984) and when Müller cells lose their typical alignment, shape, und (ultra-) structure under pathological conditions such as posterior uveitis (Eberhardt et al., 2011). These observations suggest that Müller cells may be involved in intraretinal light guidance. More direct arguments stem from different experimental approaches as mentioned in the following.
If light hits the inner (vitread) surface of the retina, it enters the Müller cell endfeet which constitute the innermost retinal layer (Fig. 1). The inner and outer stem processes of these columnar cells then extend throughout the thickness of the retinal tissue (Fig. 1B) and could thus provide a substrate for wave guidance towards the photoreceptor inner segments. Assuming total internal reflection and using measured data of cell diameters and refractive indices, V parameter values of >2 (up to 4) have been calculated (Franze et al., 2007) (Fig. 10).

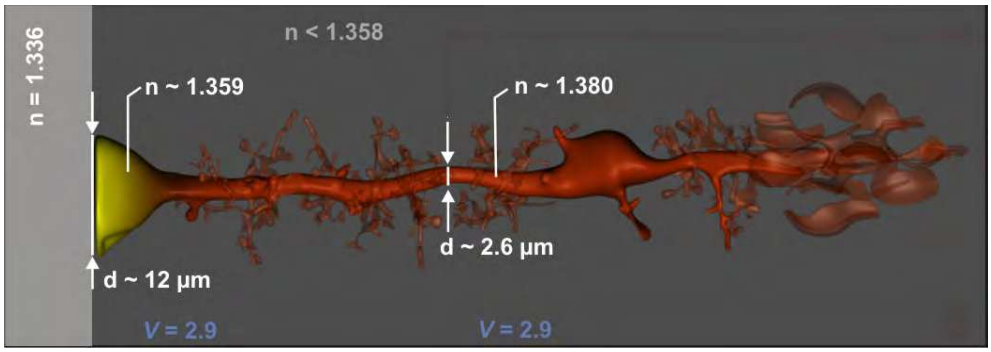

Fig. 10. Estimation of the *V* parameter along the different sectors of a typical guinea-pig Müller cell, modified from Franze et al., 2007.

While the diameter **d** of the Müller cell decreases from endfoot (left sinde; d ~ 12μm) to the stem processes (d ~ 2.6 μm), the local refractive index **n** increases from endfoot (mean n ~ 1.359; yellow) to the process (n ~ 1.380; red); thus, the ***V*** parameter remains fairly constant (2.9 for long [red] wavelengths, up to 4 for shorter [blue] wavelengths). The Müller cell endfeet constitute the boundary between the vitreous body (bright grey, n = 1.336) and the retinal neuropile (dark grey; mean n < 1.358).

Using the same assumptions and data sets, a simulation according to that shown in Figure 9B shows that Müller cell endfeet can be considered as light collectors, with a half-angle of acceptance close to 13° (similar to the cone inner segments). Moreover, the comparatively low refractive index of the innermost part of the endfeet (Fig. 10) provides index matching between the vitreous fluid and the retina, and reduces loss of light be reflection at the inner retinal surface. More detailed simulations of light propagation through human Müller cells suggest that (i) a significant increase of the intensity at the photoreceptors is obtained, (ii) for pupils up to 6 mm width, the coupling between neighboring cells is only a few percent, and (iii) low cross talk over the whole visible spectrum also explains the insensitivity to chromatic aberrations of the eye (Labin & Ribak, 2010).

In addition to these simulations, several different lines of experimental data support the view that Müller cells are light-guiding elements in the vertebrate retina. First, isolated individual cells were shown to effectively conduct light between two opposing glass fibers (cf. section 3.2 and Fig. 6). Second, the 'tubes' of low reflection spanning the vital retina, which were identified by confocal reflection microscopy, (cf. section 3.4), were shown to be the Müller cells (Fig. 11).

To understand the natural path of light through the vital retina, multiple experiments were performed in which light was applied onto the vitread surface. At this surface the Müller cell endfeet form a smooth plane covering the entire retina before they are funnelled into thick cell processes (e.g. guinea pig 2-3 μm). The tubular shape of the processes is retained until they are connected with the photoreceptor layers. Here, the Müller cell processes branch into thin cytoplasmatic arms, whose diameter is smaller than the wavelength of the visible light (Fig. 10).

In a first experiment, the inner part of the retina - or the pre-photoreceptor light path - was studied by using a multi mode optical fiber to illuminate a wide area of the retinal surface. The image, recorded at a plane close to the outer plexiform layer displays a pattern of bright spots on a dark background (Fig. 12B). This pattern represents the negative image of the image detected in the backscattering experiments. Thus, the 'tubes', which were identified as Müller cells (3.4.), transmit more of the incident light and scatter less then their surrounding structures.

To investigate the interaction between Müller cells and photoreceptor cells (i.e. the distribution of light from one Müller cell to the attached light-sensitive photoreceptor cells) the whole retina was analyzed regarding its light transmission. These experiments require a small light source to allow an illumination of individual Müller cell endfeet. For this reason, the multi mode fiber previously used was replaced by a single mode fiber. The beam waist was small enough to shine a light spot on single Müller cells. The illuminated photoreceptor cells were observed at the opposite surface (Fig. 12 C, D). These experiments revealed that the light, which enters one Müller cell, is clearly assigned to a small group of adjacent photoreceptor cells (Fig. 12C, red). When the fiber was moved along the retinal surface, the receptor groups moved in the same direction (Fig. 13). However, several fiber steps were required to achieve one 'jump' of the illuminated spot at the receptor layer. Sometimes

sideward-deviations' occurred as well as even 'backward jumps' which can be explained by the orientation of Müller cells in the tissue. In some cases, more than one group of photoreceptors were illuminated simultaneously, probably reflecting the positioning of the beam over two or three adjacent Müller cell endfeet (Fig. 13, green and 12D).

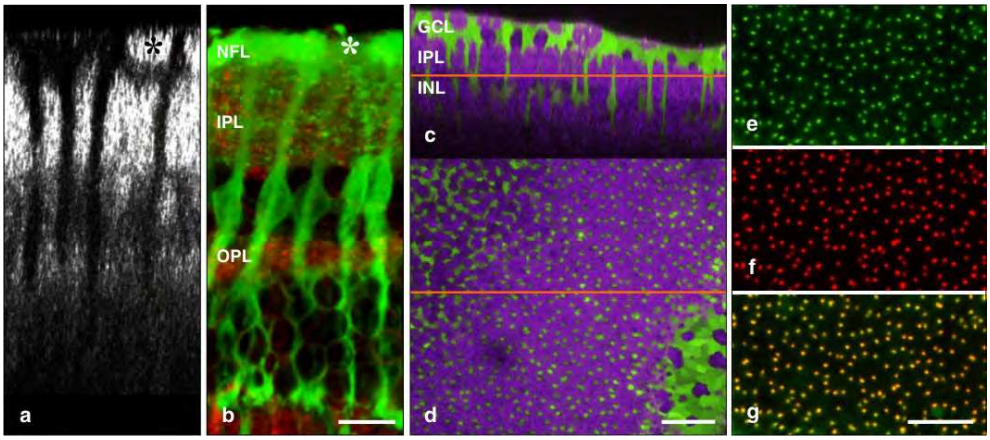

Fig. 11. Structures of low light reflection in the inner retina are Müller cells. (*a*) *Z*-reconstruction of reflection images of a living retina. Main scattering elements (bright) are the axon bundles and both plexiform layers. Low-reflecting tubular structures are spanning the entire retina. (*b*) Living retinal slice preparation, visualizing Müller cells (green) and synaptic elements in both plexiform layers (IPL, OPL) (red) (20). The levels of the IPL, OPL, and NFL (nerve fiber layer) are the same as in (*a*). The asterisks indicate axon bundles in the NFL. Scale bar, 10 µm, also valid for (*a*). (*c*, *d*) Overlay of light detected in reflection mode (purple) and the fluorescence signal of Müller cells. (*c*) Z-reconstruction of a confocal image stack. (*d*) Oblique optical section at the level of the red horizontal line in (*c*). The dye-filled irregularly shaped Müller cell somata of the inner nuclear layer (INL) are visible in the left upper corner. The central area shows Müller cell cross-sections in the inner plexiform layer (IPL). In the lower right part, Müller cell endfeet are visible, which enclose the ganglion cell somata in the ganglion cell layer (GCL). The lack of merging of the two colors, which would result in white areas, demonstrates that the dye filled exclusively those structures that showed low light reflection. (*e*-*g*) Confocal image at the IPL of a retinal wholemount fixed in 4% paraformaldehyde, after exposure to the green vital dye and immunocytochemical labeling of vimentin (red), which in the retina is specific to Müller cells (17, 22). (*e*) Fluorescence of the vital dye. (*f*) Vimentin immunofluorescence. (*g*) Overlay of (*e*) and (*f*). Colocalization of the red and green dyes results in yellow labeling. The observed complete colocalization means that the vital dye-filled and the immunoreactive cells are identical, and thus identifies the low-reflecting tubular structures as Müller cells. Scale bars in (*c*-*g*), 25 µm. Adapted from Franze et al. 2007, Copyright (2007) National Academy of Sciences, USA.

To further investigate this jumping behaviour of light, retinal cross-sections were observed while the retinal surface was again exposed to laser light emanating from a single mode optical fiber. Müller cells were fluorescently labelled, and retinae were attached to a membrane. This membrane served as a 'screen' to visualize the transmitted light. In these

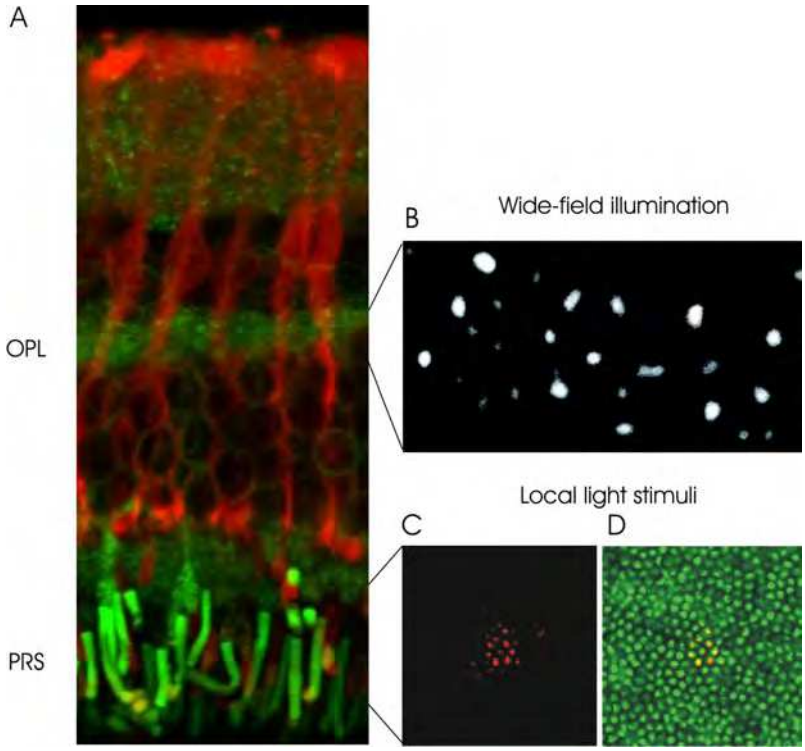

Fig. 12. Detection of light guiding structures in the retina. (A) Fluorescent image of the vital retina. Fluorescently labeled Müller cells (red) span the entire tissue. The endfeet are funnelled into the Müller cell processes, which are split in thin arms surrounding the photoreceptor nuclei. The light-sensitive segments of the photoreceptor cells are visualized by another fluorescent dye (green). (B) Wide-field illumination, provided by a multimode fiber, is used to illuminate a relatively large area of the retinal surface. At the outer plexiform layer, a pattern of brighter spots is visible. (C, D) Arrangement of the photoreceptor outer segments (green) illuminated by a multimode fiber (D). For selective illumination of individual Müller cells, the multi mode fiber is replaced by a single mode fiber. Light entering a small group of photoreceptor segments (red) is detected (C). (OPL: outer plexiform layer, PRS: photoreceptor segment layer).

experiments, (i) the position of the glass fiber, (ii) the Müller cells in the living retina, (iii) the light scattering inside the tissue, and (iv) the transmitted light were simultaneously observed. When the laser beam was not directly illuminating a Müller cell, intraretinal scattering occured mainly in the inner plexiform layer (IPL). The transmitted light at the membrane appeared as a wide spot (Fig. 14, bottom). If , however, the beam entered a Müller cell endfoot, most of the previously detected scattering inside the retina disappeared and a much narrower, bright light spot was transmitted to the photoreceptors (Fig. 14, top). Taken together, all experiments indicated that each Müller cell is optically coupled to a distinct small area in the photoreceptor layer. Further analysis has shown that the distance between the intensity maxima of these 'illuminated receptor fields' corresponds to the

average distance between the axes of two neighbouring Müller cells. This suggests that every Müller cell serves as 'optical fiber' for 'its own' group of photoreceptor cells (Agte et al., 2011). A quantitative evaluation of the photoreceptors in 'typical' mammalian retinae such as human (outside the fovea centralis), guinea pig, and others, showed that a group of 1 cone and about 10 rods belong to 1 Müller cell (Reichenbach and Robinson, 1995), suggesting that Müller cells play a central role in vision at both daylight and dawn. During night, the small amount of light is efficiently guided to the low-light sensitive rod photoreceptors. At daylight, the resolution is limited by the cone spacing. Every cone photoreceptor is equipped with its own wave guide, which thus provides high-contrast vision at daylight (Agte et al., 2011).

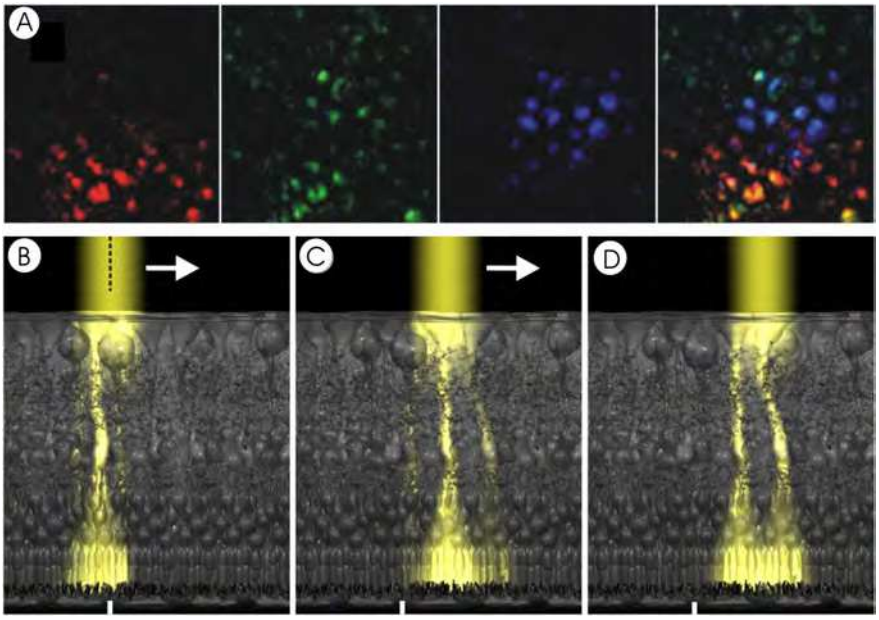

Fig. 13. Each Müller cell provides light for its own 'illuminated receptor field'. (A) When light is sent through an individual Müller cell, a distinct group of bright dots appears at the level of the outer segments (red). Movement of the light source relative to the inner retinal surface results in a 'jumping' of discrete illuminated fields at the backside of the tissue. (B, C, D) Schemata of the light behaviour inside the retina explaining the effect observed in (A). (B) The light beam illuminates a single Müller cell endfoot, which results in a single 'illuminated receptor field'. (C) A fiber step moves the beam in front of another Müller cell and another group of receptors is addressed. In this position the coupling of light into adjacent Müller cells is less efficient. (D) The beam above the edge of two neighbouring Müller cells results in a simultaneous detection of two receptor fields.

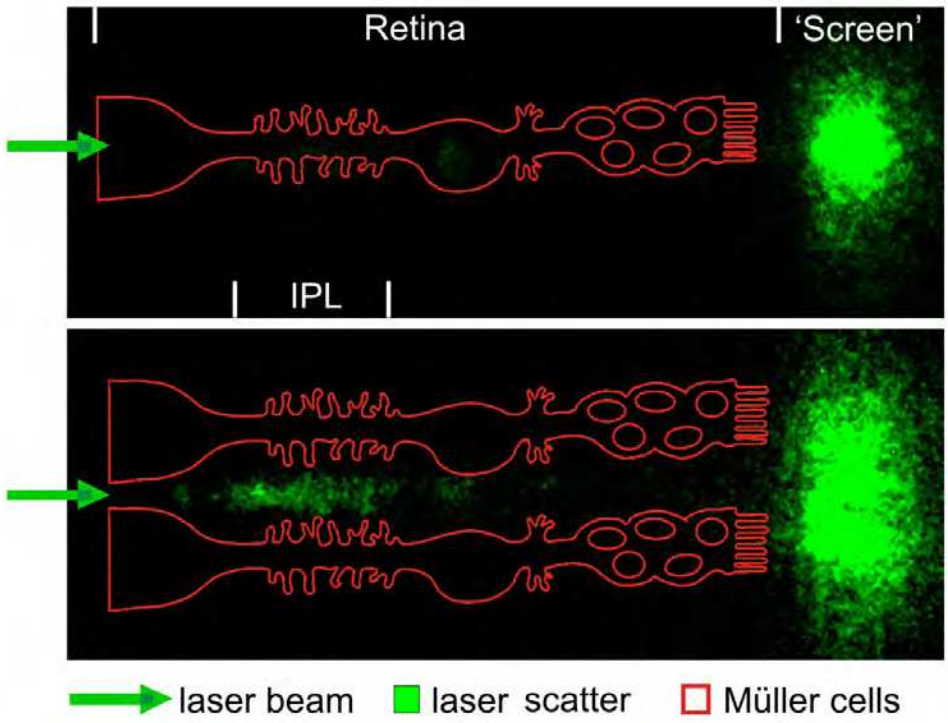

Fig. 14. Visualization of the light path within vital retinal slices. The retina is attached to a nitrocellulose membrane. A micromanipulator horizontally positions a single mode fiber in front of the vitread surface. This assembly is placed under the objective of an confocal microscope to detect the light scattering inside the retinal tissue as well as the transmitted light at the membrane. The membrane serves as a 'screen' for the light after passing the retina. In a position where the fiber is placed between two Müller cell processes (bottom) light scattering occurs particularly in the inner plexiform layer (IPL). The transmitted light spot at the membrane covers a wide area. For a better impression of the situation, Müller cell positions are schematically indicated (red line). If the laser beam hits a Müller cell endfoot (top) the scattering of light in the retina decreases and the light spot at the membrane shows rather sharp boundaries as well as a smaller spot size, suggesting that Müller cells relay light through the inner retina.

4.3 The 'special case': chains of cell nuclei act as 'microlense arrays' in the outer retina of nocturnal mammals

Nocturnal mammals such as mice and rats possess retinae with very high rod photoreceptor cell densities which increase light sensitivity by an optimal absorption probability of photons at low intensity levels. However, it requires the piling of rod somata, which mainly contain the nuclei, in many rows (10 or more). An extraordinary high degree of heterochromatin condensation reduces the size of nuclei and somata. In contrast, retinae of mammals with diurnal or crepuscular life style (such as those of horses, guinea pigs, and rabbits) display lower rod densities; their ONL contains few layers of somata / nuclei (2-5) and their rod nuclei

appear less dense. The thick ONL in retinae of nocturnal mammals appears to be a particular challenge for effective light propagation, because the Müller cell processes in the ONL are thin and irregularly shaped such that they probably cannot act as wave guides. Recently, it has been shown that the disadvantage of an elongated light path may be compensated by improved optical properties of the condensed nuclei, acting as perfect chains of lenses (Solovei et al., 2009) (Fig. 15). Also in this instance have the experimental findings be supported by thorough theoretical modelling, taking into account the wave nature of light (Kreysing et al., 2010). Noteworthy, Müller cells may play an indirect role in this mechanism because they help to align the stacks of photoreceptor somata (Fig. 1).

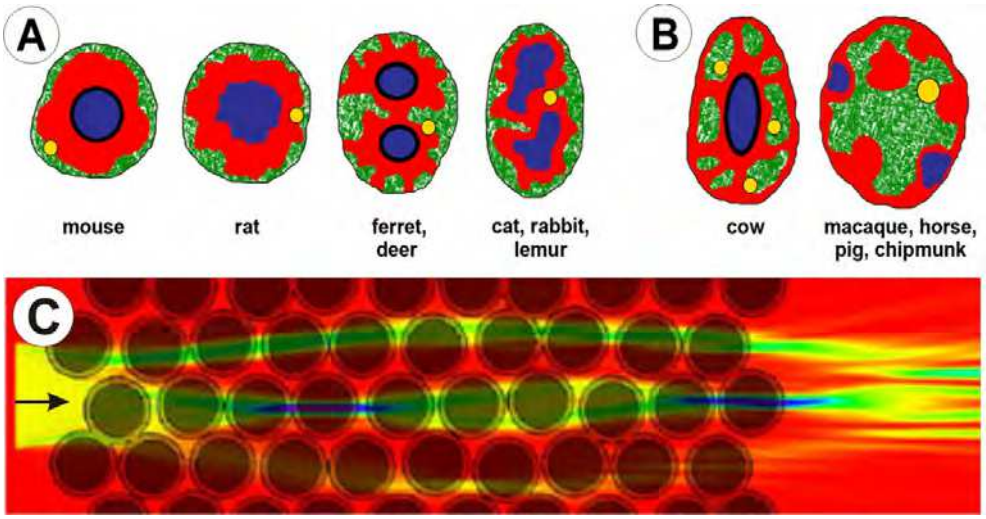

Fig. 15. Stacks of rod photoreceptor nuclei may act as light-guiding chains of lenses in nocturnal mammals. A, B: Distribution of euchromatin (green) and heterochromatin (red & blue) in rod photoreceptor cell nuclei of several mammals: A: nocturnal species, B: diurnal species; The nucleoli are labeled in yellow. C: Simulation of light propagation through the columnar stacks of rod cell nuclei in the outer nuclear layer, considered as chains of optical lenses. In this simulation, a light beam is entering from left side (arrow), i.e. from the outer plexiform layer; the inner and outer segments of the photoreceptors would be illuminated at the right side. Modified from Solovei et al. (2009).

4.4 The vertebrate retina consists of several 'stacks' of arrays of light-guiding elements

Taken together, the vertebrate retina apparently consists of several successive arrangements of vital light-guiding live 'optical fibers' or light-guiding elements that compensate the disadvantages of the inverted structure. To give an impression of the full-length light path through the retina, Figure 16 summarizes the available data and hypotheses. It has long been accepted that both the outer and the inner segments of the photoreceptors display the properties of wave guides (section 4.1). More recently, the Müller cells (section 4.2) and the nuclei of the photoreceptor cells (section 4.3) were suggested to contribute to intraretinal light propagation. This leaves us with not less than 4 subsequent components of a light-

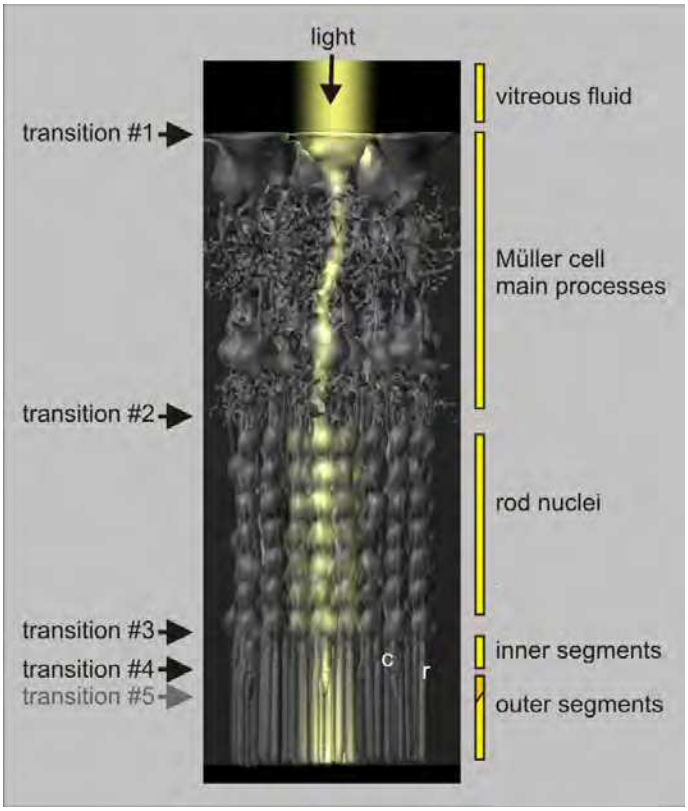

Fig. 16. Artist's view of the light path through the vertebrate retina. After being projected through the vitreous body, light is further transmitted by (i) the Müller cell stem processes, (ii) the rows of photoreceptor cell nuclei, (iii) the inner segments, and (iv) the outer segments of photoreceptor cells. This involves four transition sites, (1) from vitrous to Müller cell endfeet, (2) from Müller cell outer stem process to rod nuclei, (3) from photoreceptor cell nuclei to inner segments, and (4) from inner to outer segments. An additional transition from (peripheral) cone to rod outer segments (#5) has been proposed. c, cone; r, rod.

guiding pathway from the inner retinal surface to the end of the photoreceptor outer segments (Fig. 16). In addition to these 4 components (which differ in their light-guiding parameters and even mechanisms), the scenario involves the occurrence of (at least) 4 'transition sites'.

At first place, light arriving via the vitreous fluid must enter the retina. As the inner retinal surface (below a basal lamina) is formed by the endfeet of the Müller cells, these structures must constitute the site of this transition (see also section 4.2). The next transition is supposed to occur at the border between the OPL and the ONL, i.e., between the tapering Müller cell stem processes and the rod nuclei. Not much is known about the detailed (ultra-) structure of this transition zone, and about possible mechanisms of light transport at this site. Subsequently, at the third transition zone light must pass from the nuclear stacks to the inner segments of photoreceptor cells, close to the OLM. It has been argued that the inner

segments of photoreceptors (particularly, of the cones) are well-suited to function as light-collectors (Winston and Enoch, 1971) which may facilitate this transition. The fourth 'obligatory' transition occurs between the inner and outer segments of the photoreceptors. These structures are connected by a very thin cilium (well below the wavelength of visible light) which certainly cannot function as a light-guiding fiber with total internal reflection. This transition has never been discussed in detail. It should be noted, however ,that considerable backscattering of light seems to occur at the level of the cilia, in optical coherence tomography of the human retina (Anger et al., 2004).
Finally, an additional ('facultative') transition has been proposed by Miller and Snyder (1973). These authors suggested that light that was not absorbed in the short, tapering outer segments of the cones may spread from there towards the (longer) outer segments of the rods. This pathway was explained by the 'light radiator' properties of the peripheral cone outer segments (see Fig. 9C, *light radiator*).

5. Open questions

Although the above-mentioned experiments and models provided some indication for the presence of 'live optical elements' in the vertebrate retina, some open questions remain. For instance,

- there might be other mechanisms involved than classical wave guidance in optical fibers, such as for instance, microcrystal guidance;
- it remains to be shown to what degree does light transport by retinal cells improve vision / how efficient is light transport;
- light transport across the 'transition zones' between the successive arrangements of light-guiding live 'optical fibers' remains to be explained (cf. Fig. 16);
- the Müller cell population has been proposed to constitute a natural 'optical fiber plate' (Franze et al., 2007) but it remains to be clarified whether the ocular optics (cornea, lens, etc) focus the images onto the inner retinal surface or onto the photoreceptor layer;
- Müller cell light guidance as discussed above is supposedly in conflict with the small-eye effect (Glickstein and Millodot, 1970) and the Stiles-Crawford effect (Enoch & Tobey, 1981); this remains to be resolved (also requiring a careful reinterpretation of the original experimental evidence from the older studies in the light of the new findings;
- it remains to be shown whether all Müller cells in all vertebrates are light guides; in many (non-mammalian, or nocturnal mammalian) species the Müller cells, or parts of them, are very thin (< 0.3 μm in diameter) and thus appear not to be suitable as wave guides, at least for 'classical' total reflection.
- cells are active systems: can cells in the retina regulate light transport?;

These (and other) open questions must remain subject of future studies.

6. Conclusion

Often the retina is considered as a transparent tissue through which light passes without loss or scattering. However, this is not true; all cells and their processes and organelles are phase objects which differ in their refractive indices, which means that they must scatter the light. In particular, the synapses in the two plexiform layers have diameters close to 500nm, i.e., within the range of visible light (ca. 400-700nm). Indeed, light scattering by the retinal tissue layers is evidenced by the mere fact that optical coherence tomography delivers

images of these layers in the living eye (cf. Fig. 4). Thus, the inverted structure of the vertebrate retina has prompted the question how it is possible that we see sharp, unblurred images at daylight, and can detect a few photons entering our eye (Pirenne, 1967). The presence of light-scattering elements in front of our photoreceptor cells should decrease both visual acuity and light sensitivity. An explanation can be provided by the existence of light-guiding elements that traverse all retinal layers, and directly transfer the light (and the image of the environment) towards the light-absorbing outer segments of the photoreceptor cells. Here we summarize evidence supporting the view that the vertebrate retina apparently consists of several successive arrangements of such 'optical elements' that compensate for the disadvantages of the inverted structure (Fig. 16). There are 4 subsequent components of a light-guiding pathway from inner retinal surface to the end of the photoreceptor outer segments, i.e., Müller cells, stacks of photoreceptor cell nuclei (only in nocturnal mammals?), and the inner and outer segments of the photoreceptor cells. These 4 components, which differ in their light-guiding parameters and the underlying mechanisms, must be 'bridged' by at least 4 'transition sites'. Although many open questions remain, it appears to be very likely that cellular light guidance is a major factor in vertebrate vision.

7. References

Agte, S., Junek, S., Matthias, S., Ulbricht, E., Erdmann, I., Wurm, A., Schild, D., Käs, J.A., & Reichenbach, A. (2011). Müller glial cell-provided cellular light guidance through the vital mammalian retina. *Biophys J* accepted

Ajo, A. (1949). On the refractive index of the retina. *Acta Physiol. Scand.,* Vol. 13, No. 1-2, (Feb. 1947), pp. 130-149, ISSN 1748-1708

Anger, E.M., Unterhuber, A., Hermann, B., Sattmann, H., Schubert, C., Morgan, J.E., Cowey, A., Ahnelt, P.K, & Drexler, W. (2004). Ultrahigh resolution optical coherence tomography of the monkey fovea. Identification of retinal sublayers by correlation with semithin histology sections. *Exp. Eye Res.,* Vol. 78, No. 6, (Jun. 2004), pp. 1117-1125, ISSN 0014-4835

Barer, R. (1954) Refractometry of living cells. *Q. J. Microsc. Sci*., Vol. 95, No. 4, (Dec. 1954), pp. 399-423, ISSN 0370-2952

Bass, M. (1995) Handbook of Optics, Volume I: Fundamentals, Techniques, and Design (2nd ed.), McGraw-Hill, ISBN 9780070477407, USA

Boehm, G. (1940). Über ein neues entoptisches Phänomen im polarisierten Licht. „Periphere" Polarisationsbüschel. *Acta Ophthalmol.,* Vol. 18, No. 2, (Sep. 1940), pp. 143-169, ISSN 1755-375X

Charman, W.N. (1980). Reflection of plane-polarized light by the retina. *Bri.t J. physiol. Opt.*,Vol. 34, (1980) pp. 34-41., ISSN 0007-1218

Charriere, F., Marian, A., Montfort, F., Kuehn, J., Colomb, T., Cuche, E., Marquet, P., & Depeursinge, C. (2006). Cell refractive index tomography by digital holographic microscopy. *Opt. Lett.,* Vol. 31, No. 2, (Jan. 2006). pp. 178-180, ISSN 0146-9592

Chen, E. (1993). Refractive indices of the rat retinal layers. *Ophthalmic Res.*, Vol. 25, No. 1, (Jan./Feb. 1993), pp. 65-68, ISSN 0030-3747

Coletta, N.J., Williams, D.R., & Tiana, C.L.M. (1990). Consequences of spatial sampling for human motion perception. *Vision Res.*, Vol. 30, No. 11, (1990), pp. 1631-1648, ISSN 0042-6989

De Oliveira Castro, G., Martins-Ferreira, H., & Gardino, P.F. (1985). Dual nature of the peaks of light scattered during spreading depression in chick retina. *An Acad. bras Cienc.*, Vol. 57, No. 1, (Mar. 1985), pp. 95-103, ISSN 0001-3765

Eberhardt, C., Amann, B., Feuchtinger, A., Hauck, S.M., & Deeg, C.A. (2011). Differential expression of inwardly rectifying K+ channels and aquaporins 4 and 5 in autoimmune uveitis indicates misbalance in Müller glial cell-dependent ion and water homeostasis. *Glia*, Vol. 59, No. 5, (May 2011), pp. 697-707, ISSN 0894-1491

Enoch, J.M. (1961). Visualization of wave-guide modes in retinal receptors. *Am. J. Ophthalmol., Vol.* 51, (May 1961), pp. 1107-1118, ISSN 0002-9394

Enoch, J.M., & Tobey, F.L. (1978). Use of the waveguide parameter V to determine the difference in the index of refraction between the rat rod outer segment and the interstitial matrix. *J. Opt. Soc. Am.*, Vol. 68, No. 8, (Aug. 1978), pp. 1130-1134, ISSN 1084-7529

Enoch, J.M., & Tobey, F.L. (1981). Vertebrate Photoreceptor Optics (1st ed.), Springer Verlag, ISBN 9783540105152, Berlin-Heidelberg-New York

Enoch, J.M., & Glismann, L.E. (1966). Physical and optical changes in excised retinal tissue. Resolution of retinal receptors as a fiber optic bundle. *Invest. Ophthamol. Vis. Sci., Vol.* 5, No. 2 (Apr. 1966), pp. 208-221, ISSN 0146-0404

Franze, K., Grosche, J., Skatchkov, S.N., Schinkinger, S., Foja, C., Schild, D., Uckermann, O., Travis, K., Reichenbach, A., & Guck, J. (2007). Müller cells are living optical fibers in the vertebrate retina. *Proc. Natl. Acad. Sci. U S A*, Vol. 104, No. 20, (May 2007), pp. 8287-8292, ISSN 0027-8424

Glickstein, M., & Millodot, M. (1970). Retinoscopy and eye size. *Science*, Vol.168, No. 931, (May 1970), pp. 605-606. ISSN 0036-8075

Goldsmith, T.H. (1990). Optimization, constraint, and history in the evolution of eyes. *Quarterly Rev. Biol.*, Vol. 65, No. 3, (Sep. 1990), pp. 285-287, ISSN 0033-5770

Gorrand, J-M. (1986). Separation of the reflection by the inner limiting membrane. *Ophthalmic Physiol. Opt.*, Vol. 6, No. 2, (Apr. 1986) pp. 187-196, ISSN 0275-5408

Gouras, P. (1958). Spreading Depression of Activity in Amphibian Retina. *Am. .J Physiol.*, Vol. 195, No. 1, (Oct. 1958), pp. 28-32, ISSN 0002-9440

Hammer, M., Roggan, A., Schweitzer, D., Müller, G. (1995). Optical properties of ocular fundus tissues-an in vitro study using the double-integrating-sphere technique and inverse Monte Carlo simulation. *Phys. Med. Biol.*, Vol. 40, No. 6, (Jun. 1995), pp. 963-978, ISSN 0031-9155

Jean, J., & O'Brian, B. (1949). Microwave test of a theory of the Stiles-Crawford effect. *J. Opt. Soc. Amer., Vol.* 39, No. 9, (1949), p. 1957, ISSN 1084-7529

Kreysing, M., Kießling, T., Fritsch, A., Dietrich, C., Guck, J., & Käs, J. (2008). The optical cell rotator. *Opt. Express* , Vol. 16, No. 21, (Oct. 2008), pp. 16984-16992, ISSN 1094-4087

Kreysing, M., Boyde, L., Guck, J., & Chalut, K.J. (2010). Physical insight into light scattering by photoreceptor cell nuclei. *Opt. Lett.*, Vol. 35, No. 15, (Aug. 2010), pp. 2639-2641, ISSN 0146-9592

Knighton, R.W., Jacobson, S.G., & Kemp, C.M. (1989). The spectral reflectance of the nerve fiber layer of the macaque retina. *Invest. Ophthalmol. Vis. Sci.*, Vol. 30, No. 11, (Nov. 1989), pp. 2393-2402, ISSN 0146-0404

Labin, A.M., & Ribak, E.N. (2010). Retinal glial cells enhance human vision acuity. *Phys Rev Lett.*, Vol. 104, No. 15, (Apr. 2010), pp. 158102, ISSN 0031-9007

Livingstone, M., & Hubel, D. (1988). Segregation of form, color, movement, and depth: anatomy, physiology, and perception. *Science*, Vol. 240, No. 4853, (May 1988), pp. 740-749, ISSN 0036-8075

Martins-Ferreira, H., & De Castro, O.G. (1966) Light-scattering changes accompanying spreading depression in siolated retina. *J. Neurophysiol*., Vol. 29, No. 4, (Jul. 1966), pp. 715-726, ISSN 0022-3077

Miller, W.H., & Snyder, A.W. (1973). Optical function of human peripheral cones. *Vision Res*., Vol. 13, No. 12, (Dec. 1973), pp. 2185-2194, ISSN 0042-6989

Millodot, M. (1972). Reflection from the fundus of the eye and its relevance to retinoscopy. *Atti Fond. G. Ronchi., Vol.* 27, No. 1, (1972), pp. 31-50, ISSN 0391-2051

Mori, S., Miller, W.H., & Tomita, T. (1976). Müller cell function during spreading depression in frog retina. *Proc. Natl. Acad. Sci. U S A*, Vol. 73, No. 4, (Apr. 1976), pp. 1351-1354, ISSN 0027-8424

Nordenson, J.W. (1934). Über den Brechungsindex der Netzhaut. *Acta Ophthalmol. Copenhagen,* Vol. 12, (1934), pp. 171-175, ISSN 0001-639X

Pirenne, M.H. (1967). Vision and the Eye (2nd ed.), Chapman and Hall Ltd., ISBN 9780412042201, London, (and references therein)

Puliafito, C.A., Hee, M.R., Lin, C.P., Reichel, E., Schuman, J.S., Duker, J.S., Izatt, J.A., Swanson, E.A., & Fujimoto, J.G. (1995). Imaging of macular diseases with optical coherence tomography. *Ophthalmol*., Vol. 102, No. 2, (Feb. 1995), pp. 217-229, ISSN 0161-6420

Reichenbach, A., & Robinson, S. (1995). Phylogenetic constraints on retinal organization and development. *Progr. Retin. Eye Res., Vol.* 15, No. 1, (1995), pp. 139-171, ISSN 1350-9462

Sidman, R.L. (1957). The structure and concentration of solids in photoreceptor cells studied by refractometry and interference microscopy. *J. Biophys. and Biochem. Cytology*, Vol. 3, No. 1, (Jan. 1957), pp. 15-30, ISSN 0095-9901

Solovei, I., Kreysing, M., Lanctôt, C., Kösem, S., Peichl, L., Cremer, T., Guck, J., & Joffe, B. (2009) Nuclear architecture of rod photoreceptor cells adapts to vision in mammalian evolution. *Cell, Vol.* 137, No. 2, (Apr. 2009), pp. 356-68. ISSN 0092-8674

Tobey, F.L., Enoch, J.M., Scandrett, J.H. (1975). Experimentally determined optical properties of goldfish cones and rods. *Invest. Ophthalmol, Vol.* 14, No. 1, (Jan. 1957), pp. 7-23, ISSN 0020-9988

Valentin, G. (1879). Ein Beitrag zur Kenntniss der Brechungsverhältnisse der Thiergewebe. *Arch. ges. Physiol*., Vol. 19, No.1 (Dez. 1879), pp. 78-105, ISSN 0365-267X

van Harreveld, A. (1984) Visual concomitants of retinal spreading depression. *Ann. Acad. Brasil. Ciênc*., Vol. 56, No. 4, (Dec. 1984), pp. 519-524, ISSN 0001-3765

Vos, J.J., & Bouman, M.A. (1964). Contribution of the retina to entoptic scatter. *J. Opt. Soc. Am*., Vol. 54, No. 1, (Jan. 1964), pp. 95-100, ISSN 1084-7529

Williams, D., Sekiguchi, N., & Brainard, D. (1993). Color, contrast sensitivity, and the cone mosaic. *Proc. Natl. Acad. Sci. U S A*., Vol. 90, No. 21, (Nov. 1993), pp. 9770-9777, ISSN 0027-8424

Winston, A., & Enoch, J.M. (1971). Retinal cone receptor as an ideal light collector. *J. Opt. Soc. Am*., Vol. 61, No. 8, (Aug. 1971), pp. 1120-1122, ISSN 1084-7529

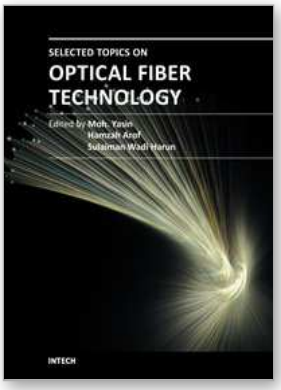

Selected Topics on Optical Fiber Technology

Edited by Dr Moh. Yasin

ISBN 978-953-51-0091-1

Hard cover, 668 pages

Publisher InTech

Published online 22, February, 2012

Published in print edition February, 2012

This book presents a comprehensive account of the recent advances and research in optical fiber technology. It covers a broad spectrum of topics in special areas of optical fiber technology. The book highlights the development of fiber lasers, optical fiber applications in medical, imaging, spectroscopy and measurement, new optical fibers and sensors. This is an essential reference for researchers working in optical fiber researches and for industrial users who need to be aware of current developments in fiber lasers, sensors and other optical fiber applications.

InTech Europe
University Campus STeP Ri
Slavka Krautzeka 83/A
51000 Rijeka, Croatia
Phone: +385 (51) 770 447
Fax: +385 (51) 686 166
www.intechopen.com

InTech China
Unit 405, Office Block, Hotel Equatorial Shanghai
No.65, Yan An Road (West), Shanghai, 200040, China
中国上海市延安西路65号上海国际贵都大饭店办公楼405单元
Phone: +86-21-62489820
Fax: +86-21-62489821